Structural and morphological studies on SiO_xN_y thin films

D. Criado [a,*], A. Zúñiga [b], I. Pereyra [a]

[a] EPUSP, University of São Paulo, CEP 5424-970, CP 61548 São Paulo, SP, Brazil
[b] Departamento de Ingeniería Mecánica, Facultad de Ciencias Físicas y Matemáticas, Universidad de Chile, Beauchef 850, Santiago, Chile

Abstract

In this work, the structure and morphology of silicon oxynitride films deposited by the PECVD technique were studied. The films were deposited under two different conditions: (a) SiO_xN_y with chemical compositions varying from SiO_2 to Si_3N_4 via the control of a $N_2O + N_2 + SiH_4$ gas mixture, and (b) Si-rich SiO_xN_y films via the control of a $N_2O + SiH_4$ gas mixture. The analyses were performed using X-ray near edge spectroscopy (XANES) at the Si-K edge, transmission electron microscopy (TEM) and Rutherford backscattering spectroscopy (RBS). For samples with chemical composition varying from SiO_2 to Si_3N_4, the diffraction patterns obtained by TEM exhibited changes with the chemical composition, in agreement with the XANES results. For silicon-rich silicon oxynitride samples, the formation of a-Si clusters was observed and the possibility of obtaining Si nanocrystals after annealing depending on the composition and temperature was realized.

Keywords: Silicon; Chemical vapor deposition; Plasma deposition; Atomic absorption; Rutherford backscattering; STEM/TEM; TEM/STEM; X-ray absorption

1. Introduction

Silicon oxynitride (SiO_xN_y) films have been widely studied for their use in the new generation of microelectronic and optoelectronic devices due to the ability of controlling their optical and electrical properties through the adjustment of the chemical composition [1,2].

Since SiO_xN_y is a ternary alloy, it possesses a complex structure; thus, a detailed knowledge about the structure and morphology of SiO_xN_y films becomes essential for the improvement of optical and microelectronic devices. The stoichiometric silicon oxynitride, given by the formula Si_2ON_2, is a compound governed by the Mott rule [3–5], where each Si atom is fourfold-coordinated with four O and/or N atoms [4,5]. In the case of non-stoichiometric silicon oxynitride (SiO_xN_y), as for all tetrahedral amorphous non-stoichiometric alloys, two different models can describe its structure, the random bonding (RBM) and the random mixture (RMM) models. The RMM assumes that a-SiO_xN_y films are formed by a mixture of two phases: SiO_2 and Si_3N_4. The RBM, on the other hand, considers that these materials are constituted by Si–O and Si–N bonds coordinated in five types of tetrahedral: SiO_vN_{4-v} where $v = 0, 1, 2, 3, 4$ [3–5]. In the case of Si-rich material Si–Si bonds are also present and thus the permitted tetrahedra are of the type $SiSi_jO_kN_{4-(j+k)}$ where $j, k = 0, 1, 2, 3, 4$ and $j + k \leqslant 4$. For some applications such as MOS transistors, capacitors and waveguides it is necessary a homogeneous film, related to RBM, to not change the dielectric constant or the refractive index damaging the device performance. On the other hand, for LED's devices, the visible PL at room temperature in Si-rich oxynitride films has been attributed to the presence of amorphous silicon clusters in the film, better explained by the RMM model [6].

In this work SiO_xN_y films with chemical compositions varying from SiO_2 to Si_3N_4, as well as Si-rich SiO_xN_y films were deposited by PECVD at low temperature. The struc-

* Corresponding author. Tel.: +55 11 3091 5256; fax: +55 11 3091 5585.
E-mail address: dcriado@lme.usp.br (D. Criado).

0022-3093/$ - see front matter © 2007 Elsevier B.V. All rights reserved.
doi:10.1016/j.jnoncrysol.2007.09.063

ture of the materials was studied using X-ray absorption near edge spectroscopy (XANES) at the Si-K edge, high resolution transmission electron microscopy (HRTEM) and Rutherford backscattering spectroscopy (RBS).

2. Experimental

The SiO_xN_y films studied in this work were deposited in a standard 13.56 MHz RF PECVD capacitively coupled system described elsewhere [7], from appropriate gaseous mixtures of electronic grade (99.999%) silane (SiH_4), nitrous oxide (N_2O) and nitrogen (N_2).

All the samples were deposited at 320 °C, [8] and the RF power density was kept at 500 mW cm^{-2}. The SiH_4 flow was fixed at 15 sccm, value high enough to lead to appropriate deposition rates for thick films production [9], but sufficiently low to prevent undesirable gas phase reactions. The films were deposited onto p type, (1 0 0), single crystalline silicon substrates in the 1–10 Ω cm resistivity range for XANES and TEM measurements and onto ultra dense amorphous carbon for RBS measurements. The thickness of the thick samples was determined with a Tencor 500 profilometer and the samples were deposited with approximately 400 nm in thickness for TEM and XANES analyses, and with 100 nm for RBS measurements. The materials were deposited according to the conditions presented in Table 1.

The RBS experiments were performed at the LAMFI/USP, São Paulo, using a He^+ beam with 2.4 MeV of energy, charge of 30 C, current of 30 nA and detection angle of 170°. The XANES measurements were conducted at the SXS beamline [10] of the Brazilian Synchrotron Light Laboratory (LNLS, Campinas, Brazil) in the 1835–1855 eV range with 0.2 eV steps using a channel cut InSb (1 1 1) monochromator. The spectra were collected at the Si-K edge with total electron yield (TEY) detection mode. The HRTEM analyses were performed at the Transmission Electron Microscopy Laboratory, University of Chile, using a FEI Tecnai F20 microscope operated at 200 keV. The annealing treatments were performed under vacuum.

Table 1
Deposition conditions and chemical composition of all samples studied

	Gaseous mixture (sccm)	Si (%)	O (%)	N (%)
	SiH_4:H_2			
a-Si	3:100	100	0	0
	N_2O:SiH_4			
SiO_2	75:15	33	66	0
	N_2:SiH_4			
Si_3N_4	75:15	43	0	57
	N_2O:N_2:SiH_4			
SiO_2-type	60:15:15	33	65	2
Si_3N_4-type	4:71:15	36.5	22	41.5
	N_2O:SiH_4			
Silicon-rich	3.8:15	65	16	19
	7.5:15	47	27	26
	11.3:15	43	32	25

3. Results

It was observed in a previous work that using a $N_2O + N_2 + SiH_4$ gaseous mixtures it is possible to obtain films with chemical compositions varying from SiO_2 to Si_3N_4 [11]. The XANES results at the Si-K edge for as-deposited samples with chemical compositions varying from SiO_2 to Si_3N_4 are shown in Fig. 1(a). The Si-K edge of the sample produced with the highest N_2 flow is very close to that of Si_3N_4. Similarly, as the N_2 flow decreases, the absorption edge shifts towards that of SiO_2; behavior attributed to an increase in the number of Si–O bonds and a decrease in the number of Si–N bonds. The spectra corresponding to the three samples deposited with the higher N_2 flow values exhibited a second structure at an energy value intermediate between the SiO_2 and Si_3N_4 edges, which can be related to a second absorption edge. This second structure did not shift with N concentration, but its intensity increased as the N_2 flow decreased [12].

The XANES results at the Si-K edge of Si-rich SiO_xN_y (Si = 43, 47 and 65%) films before and after annealing are shown in Fig. 1(b)–(d), respectively. The spectra of CVD Si_3N_4 and thermal SiO_2 standard samples are also shown for comparison purposes. For the sample with Si content = 43% (Fig. 1(b)) it is observed that the as-deposited sample presented only one absorption edge, starting at energies close to that of Si–Si bonds, passing through values related to Si–N bonds until reaching the Si–O bonds. After annealing at $T = 750$ °C the spectrum did not show appreciable changes, while after annealing at $T = 850$ °C the spectrum presented two absorption edges, related to the separation of two phases: one composed by Si–O and Si–N bonds, and another one composed by Si–Si bonds. The as-deposited sample with Si content = 47% (Fig. 1(c)) presented high intensities starting from energies close to that of Si–Si bonds up to energies associated with Si–O bonds, but now exhibiting three defined absorption edges, one formed by Si–Si bond and another one by Si–O and Si–N bonds. After annealing at 1000 °C, the sample presented a better separation of these phases. The spectrum of the sample with Si = 65% (Fig. 1(d)) was similar to that of the SiO_xN_y sample with Si content = 47%, but with a higher intensity associated to Si–Si bonds. The annealing behavior of this sample was also similar to that of the sample with Si content = 47%, although presenting an even better separation of Si–Si and Si–O, Si–N bonds.

The HRTEM results for a-Si:H, Si_3N_4, and SiO_2 samples (with inserted diffraction patterns) are shown in Fig. 2. For the a-Si:H sample (Fig. 2(a)) the presence of nanocrystals 2–4 nm in size was observed, which is also evident in the diffraction pattern through the presence of well defined rings and diffraction spots. For the SiO_2 sample (Fig. 2(b)) an amorphous film was observed in the image, while the diffraction pattern, in agreement with the image, presented two diffuse rings. For the Si_3N_4 sample (Fig. 2(c)) an amorphous film and a diffraction pattern with two diffuse rings were also observed (similar to the SiO_2

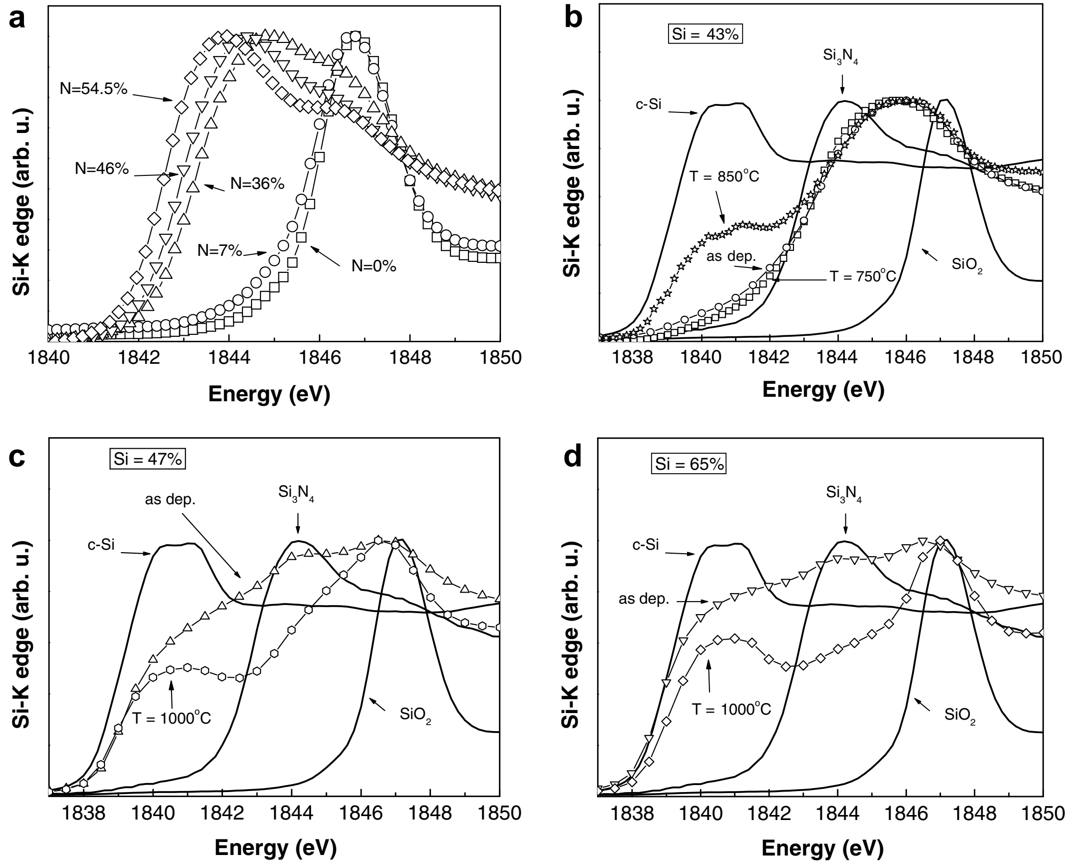

Fig. 1. XANES at Si-K edge for: (a) as deposited samples with chemical composition varying from SiO_2 to Si_3N_4. Si-rich SiO_xN_y samples with concentration of Si = (b) 43%, (c) 47% and (d) 65% before and after annealing.

sample); however, the most intense ring was closer to the image centre. In order to better compare the diffraction patterns, intensity profiles as a function of k were extracted from the experimental patterns. In Fig. 2(d) it is possible to observe that the Si_3N_4 sample presents two intensities maxima, one present at k values between 2.4 and 4.3 nm^{-1} and another one at 7.3 nm^{-1}. The SiO_2 sample also presents two intensities maxima but at different positions: at approximately 2.3 and 8 nm^{-1}, respectively. The a-Si:H film presents three maxima at approximately 3, 5 and 5.6 nm^{-1}.

In Fig. 3 the TEM results for the (a) SiO_2-like and (b) Si_3N_4-like samples are presented. Both samples presented amorphous characteristics, and the diffraction patterns of both SiO_2-like and Si_3N_4-like sample presented two diffuse rings, similar to the SiO_2 and Si_3N_4 samples. A comparison of the intensity profiles is shown in Fig. 3(c).

HRTEM images before and after annealing at 750 °C of a SiO_xN_y sample with Si = 43% are shown in Fig. 4. It can be observe that the as deposited sample (Fig. 4(a)) is amorphous and presents a diffraction pattern with two diffuse rings, similar to those of Si_3N_4. After annealing at 750 °C (Fig. 4(b)), the sample did not exhibit appreciable changes, i.e., it remained amorphous with the same intensity profile as a function of k, as shown in Fig. 4(c).

HRTEM images before and after annealing at 750 and 1000 °C of a SiO_xN_y sample with Si = 47% are shown in Fig. 5. The sample before annealing (Fig. 5(a)) was amorphous, having a diffraction pattern characterized by diffuse rings, in agreement with an amorphous material. After annealing at 750 °C (Fig. 5(b)) and 1000 °C (Fig. 5(c)), the sample did not present appreciable changes compared to the as-deposited condition, maintaining its amorphous structure. This behavior was confirmed by comparing the intensity profiles as a function of k, Fig. 5(d), where no appreciable changes can be observed after annealing.

HRTEM images before and after annealing at 750 and 1000 °C of the SiO_xN_y sample with the highest Si content, Si = 65% are shown in Fig. 6. The as-deposited sample (Fig. 6(a)) presents an amorphous structure. After annealing at 750 °C (Fig. 6(b)) it can be observed that the diffraction rings become narrower, an indication that the sample is acquiring short range order. The formation of Si nanocrystals 2–4 nm in size after annealing at 1000 °C can be observed, as shown in Fig. 6(c), in agreement with the diffraction pattern which presents well-defined diffraction rings and spots (more defined than in the sample annealed at 750 °C). In Fig. 6(d) a comparison of the diffraction intensities as a function of k for the SiO_xN_y sample with Si = 65% before and after annealing is presented. The

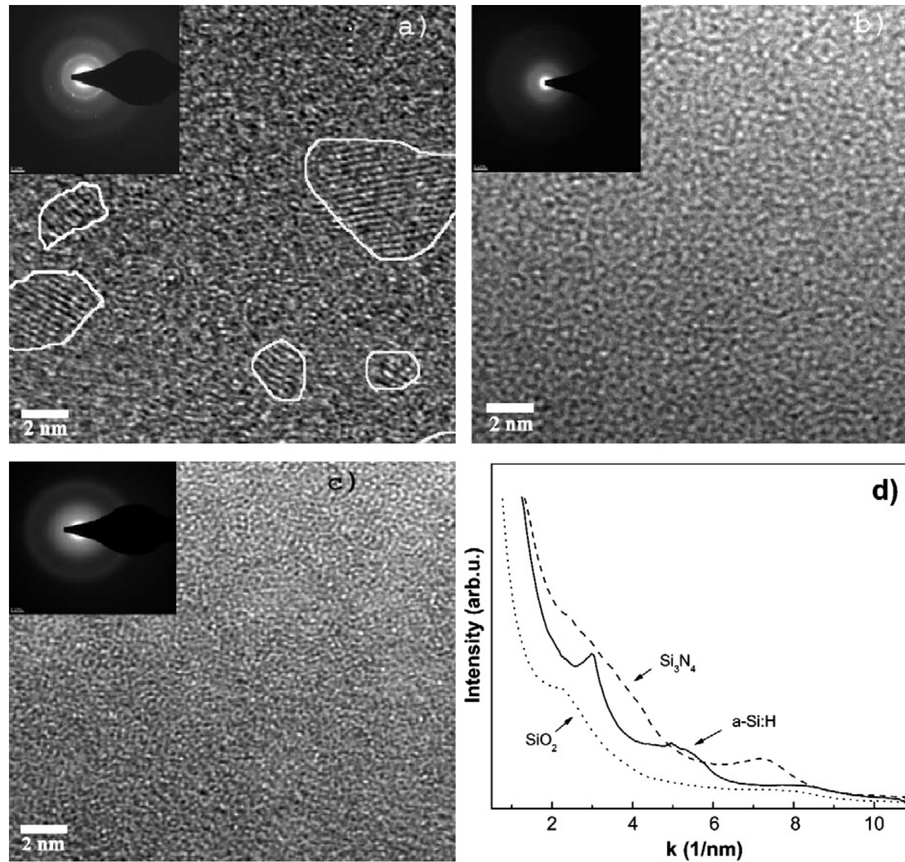

Fig. 2. TEM images with inserted diffraction patterns for the samples (a) a-Si:H, (b) SiO_2 and (c) Si_3N_4. (d) Comparison of intensities as a function of k function of a-Si:H, SiO_2 and Si_3N_4 materials.

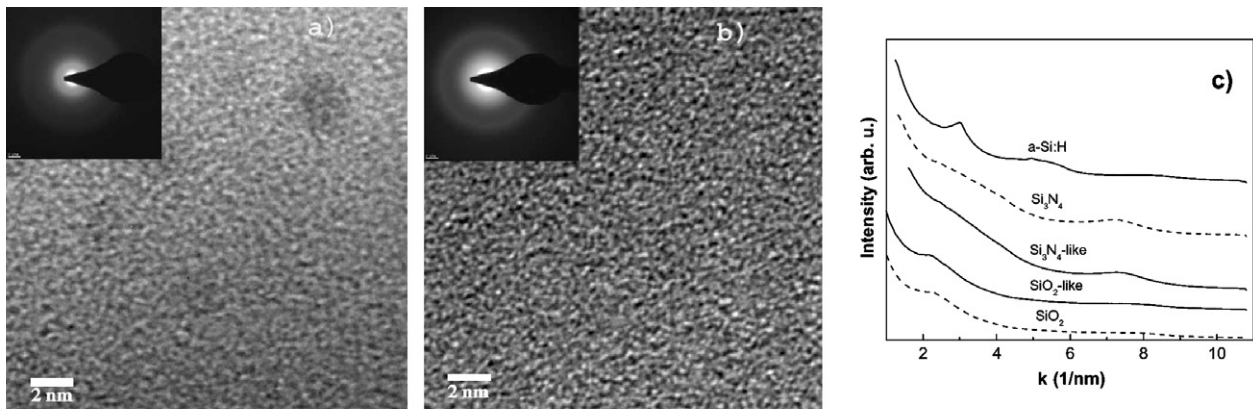

Fig. 3. TEM images with inserted diffraction patterns for the samples (a) SiO_2-like and (b) Si_3N_4-like. (c) Comparison of intensities as a function of k of SiO_xN_y samples, SiO_2 and Si_3N_4 materials.

as-deposited sample presents only two maxima of intensities at k values close to those of a-Si, i.e., at 3.07 and 5.53 nm^{-1}. After annealing at 750 °C it is shown that these intensity maxima are better defined. After annealing at 1000 °C an increase in the intensity at 3.07 nm^{-1} is observed, while the diffuse peak previously located at 5.53 nm^{-1} in the as-deposited sample splits into two peaks located at 5.25 and 6.12 nm^{-1}. These three peaks correspond to the (1 1 1), (2 2 0) and (3 1 1) planes of crystalline silicon.

4. Discussion

The XANES measurements of SiO_xN_y films deposited with $N_2O + N_2 + SiH_4$ gaseous mixtures and having a low N content, i.e. SiO_2-like, presented only one absorption edge, suggesting that under these conditions the material is better represented by the RBM model, that is to say, Si atoms bonded randomly with O and N atoms. On the other hand, films with high N content, i.e. Si_3N_4-like, presented a second structure in the absorption edge, one at

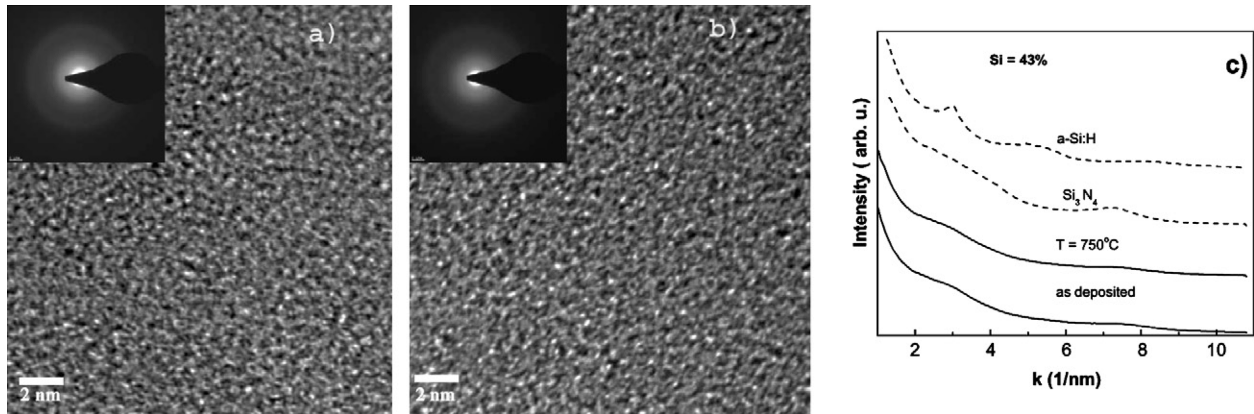

Fig. 4. TEM images with inserted diffraction patterns for the sample Si = 43% (a) before and (b) after annealing at 750 °C. (c) Comparison of intensities as a function of k of SiO_xN_y with Si = 43% and a-Si, SiO_2 and Si_3N_4 materials.

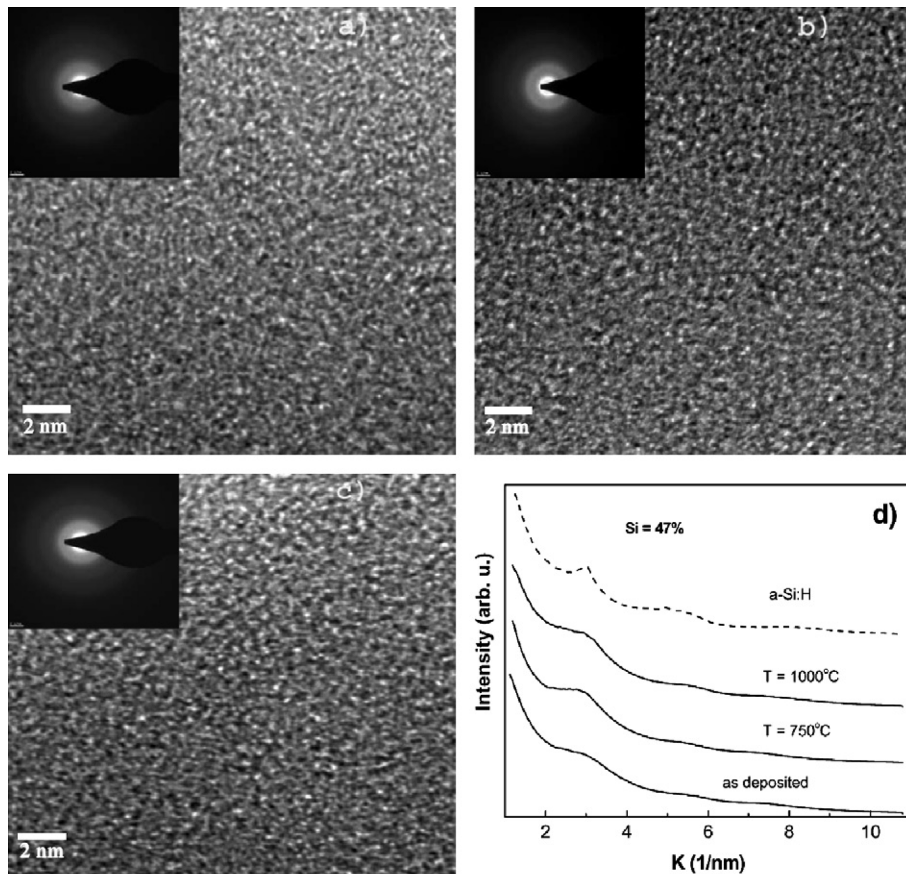

Fig. 5. TEM images with inserted diffraction patterns for the sample with Si = 47% (a) before annealing, (b) after annealing at 750 °C and (c) at 1000 °C. (d) Comparison of intensities as a function of k of SiO_xN_y with Si = 47% and a-Si, SiO_2 and Si_3N_4 materials.

lower energies related to Si_3N_4 and another at higher values close to that of SiO_2 [11,13]. This hypothesis is compatible with other author's results [14] which describe a silicon oxynitride sample having an intermediate stoichiometry by a combination of the RBM and RMM models. This material cannot described by the RBM model only due to the instability of the $Si_{2,2}$ tetrahedron caused by the electronegativity adjustment, which leads to preferential formation of $Si_{1,3}$ and $Si_{3,1}$ tetrahedra (where $Si_{n,m}$ are the number of oxygen and nitrogen atoms, respectively). The TEM investigations revealed that all samples were composed of one phase (an amorphous phase), while the diffraction patterns analysis revealed that the intensity profiles of the samples were in agreement with their chemical compositions (SiO_2-like and Si_3N_4-like samples presented intensity profiles similar to SiO_2 and Si_3N_4, respectively). However, the two phases observed with XANES in Si_3N_4-like samples could not be identified in the TEM, possibly because

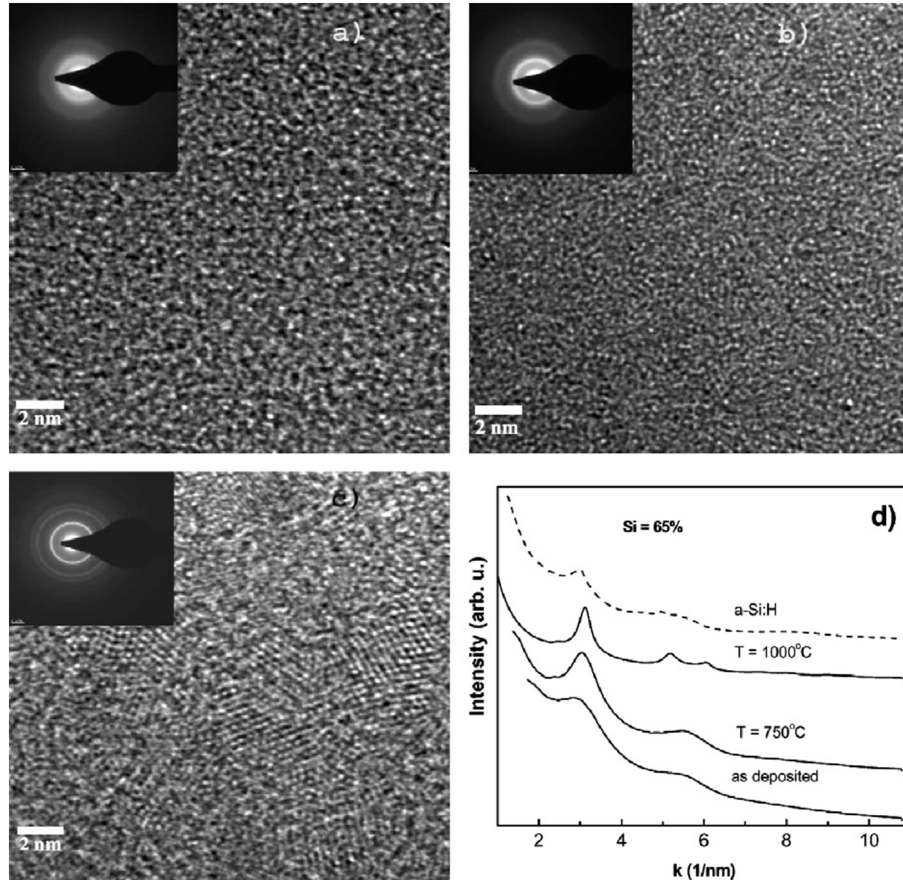

Fig. 6. TEM images with inserted diffraction patterns for the sample with Si = 65% (a) before annealing, (b) after annealing at 750 °C and (c) at 1000 °C. (d) Comparison of intensities as a function of k of SiO_xN_y with Si = 65% and the a-Si profile.

of the low contrast between these two amorphous phases with similar atomic numbers.

For Si-rich SiO_xN_y samples deposited with $N_2O + SiH_4$ gaseous mixtures XANES analyses showed that the silicon content plays an important role in relation to the structure and thermal stability. The sample with Si = 43% presented a homogeneous amorphous phase in both the as-deposited condition and after annealing at 750 °C, better represented by the RBM model. These results were confirmed by the TEM images and diffraction patterns, which showed that the sample was composed of a homogeneous amorphous phase with characteristics similar to those of Si_3N_4. This sample presented two absorption edges after annealing at 850 °C; an indication of phase separation. One of these two phases can be related to Si–Si bonds while the other one to Si–O and Si–N bonds. Therefore, the sample annealed at 850 °C can be better represented by the RMM model.

However, XANES measurements also showed that samples with Si = 47 and 65% could be better explained by the RMM model since two absorption edges were observed in the as-deposited condition, indicating the presence of one phase formed by Si–Si bonds and another one formed by Si–O and Si–N bonds. Diffraction analyses of these samples showed the presence of diffraction rings characteristic of a-Si. For samples with Si content = 47% and annealed at 750 °C and 1000 °C the XANES results showed a more organized structure revealed by an increase of the intensity of the absorption edges (phase separation), while the TEM images and diffraction patterns did not present appreciable changes. Therefore, these materials did not crystallize. A Similar result was obtained in the sample with Si content = 65% after annealing at 750 °C. However, the sample with Si content = 65% annealed at 1000 °C showed evidences of crystallization through an even more pronounced phase separation revealed by XANES, TEM images evidencing the presence of Si nanocrystals, and diffraction patterns showing the presence of well defined diffraction rings and spots corresponding to Si crystals. These results are in agreement with Raman results presented elsewhere [15], which demonstrated the presence of c-Si for that same annealed condition, but only amorphous Si–Si bonds for all the others conditions.

Although evidences of a-Si cluster formation in samples with Si content = 47 and 65% were obtained by XANES and diffraction pattern analyses, it was difficult to observe the presence of these a-Si clusters within the SiO_xN_y matrix using TEM, probably due to the similarities of densities between these materials, resulting in a very low contrast in the HRTEM image.

5. Conclusions

In this work the structure and morphology of Si-rich SiO_xN_y films and SiO_xN_y films with chemical compositions varying from SiO_2 to Si_3N_4 was investigated. The as-deposited SiO_xN_y samples with chemical composition varying from SiO_2 to Si_3N_4 were composed by a homogeneous amorphous phase as revealed by TEM. However, XANES analyses showed that SiO_2-like samples were composed of one single phase, while Si_3N_4-like samples were composed of two phases (one SiO_2-like and other Si_3N_4-like), explained by a combination of the RBM and RMM models. For Si-rich SiO_xN_y samples the possibility of obtaining a-Si clusters and Si nanocrystals through the control of the chemical composition was realized. It was also possible to correlate TEM and XANES measurements with luminescence effect measurements, allowing the optimization of these materials for optical applications.

Acknowledgements

Thanks are due to the Brazilian Synchrotron Light Laboratory – LNLS/Brazil, the Ion Beam Materials Analyze Laboratory – LAMFI-IF/Brazil for the RBS measurements, and to the Transmission Electron Microscopy Laboratory, Faculty of Physical and Mathematical Sciences, University of Chile for TEM analysis. The authors are also grateful to the Brazilian agencies FAPESP (Process Nos: 03/04523-6, 00/10027-3 and 01/06516-1) and CNPq for financial support.

References

[1] Zhenrui Yu, Mariano Aceves, Jesus Carrillo, Rosa López-Estopier, Thin Solid Films 515 (2006) 2366.
[2] Byungwhan Kim, Dong Hwan Kim, Jaeyoung Park, Seung Soo Han, Curr. Appl. Phys. 7 (2007) 434.
[3] F. Pinakidou, M. Katsikini, E.C. Paloura, Nucl. Instr. Meth. B 200 (2003) 66.
[4] V.A. Gritsenko, J.B. Xu, R.W.M. Kwok, Y.H. Ng, I.H. Wilson, Phys. Rev. Lett. 81 (1998) 1054.
[5] V.A. Gritsenko, R.W.M. Kwok, Hei Wong, J.B. Xu, J. Non-Cryst. Solids 297 (2002) 96.
[6] Sandeep Kohli, Jeremy A. Theil, Patricia C. Dippo, Richard K. Ahrenkiel, Christopher D. Rithner, Peter K. Dorhout, Thin Solid Films 473 (2005) 89.
[7] M.N.P. Carreño, J.P. Bottechia, I. Pereyra, Thin Solid Films 308 (1997) 219.
[8] I. Pereyra, M.I. Alayo, J. Non-Cryst. Solids 212 (1997) 225.
[9] M.I. Alayo, I. Pereyra, M.N.P. Carreño, Thin Solid Films 332 (1998) 40.
[10] M. Abbate, F.C. Vincentin, V. Compagnon-Cailhol, M.C. Rocha, H. Tolentino, J. Synchrotron Radiat. 6 (1999) 964.
[11] D. Criado, M.I. Alayo, I. Pereyra, M.C.A. Fantini, Mater. Sci. Eng. B 112 (2004) 123.
[12] D. Criado, M.I. Alayo, M.C.A. Fantini, I. Pereyra, J. Non-Cryst. Solids 352 (2006) 2319.
[13] D. Criado, M.I. Alayo, M.C.A. Fantini, I. Pereyra, J. Non-Cryst. Solids 352 (2006) 1298.
[14] K.-M. Behrens, E.-D. Klinkenberg, J. Finster, K.-H. Meiwess-Broer, Surf. Sci. 402-404 (1998) 729.
[15] R.A.R. Oliveira, M. Ribeiro, I. Pereyra, M.I. Alayo, Mater. Charact. 50 (2003) 161.